

Mechanism of 2,2',6,6'-Tetramethylpiperidin-*N*-oxyl-Mediated Oxidation of Alcohols in Ionic Liquids

Clement Comminges,[†] Rachid Barhdadi,[†] Andrew P. Doherty,^{*,‡} Sarah O'Toole,[‡] and Michel Troupel[†]

Institut de Chimie et des Matériaux Paris Est (ICMPE - équipe ESO), UMR 7182, CNRS - Université Paris 12, Val de Marne, 2-8 rue H. Dunant, 94320 Thiais, France, and School of Chemistry and Chemical Engineering, David Keir Building, Queen's University of Belfast, Stranmillis Road, Belfast, Northern Ireland, BT9 5AG, United Kingdom

Received: February 12, 2008; Revised Manuscript Received: May 19, 2008

The mechanism of 2,2',6,6'-tetramethylpiperidin-*N*-oxyl (TEMPO)-mediated oxidation of alcohols to aldehydes and ketones in ionic liquids has been investigated using cyclic voltammetry and rotating disk electrode voltammetry. It is shown that the presence of bases (B) and their conjugate acids (BH⁺), as well as their p*K*_as, strongly influences the rate of reaction. Data indicated that the first step in the oxidation is the formation of the alcoholate species via acid–base equilibrium with B. The alcoholate subsequently reacts with the active form of TEMPO (T⁺, i.e., the one-electron oxidized form) forming an intermediate that further reacts with T⁺ and B returning TEMPO catalytically, BH⁺, and the carbonyl product. A kinetic model incorporating this pre-equilibrium step has been derived, which accounts for the experimentally observed reaction kinetics. Overall, the rate of reaction is controlled by the equilibrium constant for the pre-equilibrium step; as such, strong bases are required for more kinetically efficient transformations using this redox catalyst.

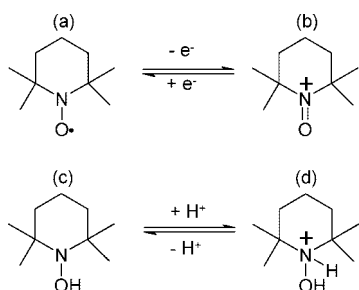


Figure 1. Structure of (a) *N*-oxyl radical T[•], (b) the *N*-oxoammonium form (T⁺), (c) the hydroxylamine form (TH), and (d) the hydroxylammonium form (TH₂⁺).

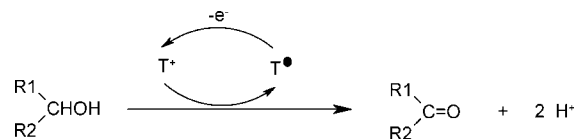
Introduction

Semmelhack et al.¹ first described the use of the *N*-oxyl radical TEMPO (Figure 1a, TEMPO = 2,2',6,6'-tetramethylpiperidin-*N*-oxyl = T[•]) as a selective and efficient redox catalyst for the electrooxidation of primary and secondary alcohols to the corresponding aldehydes and ketones.^{1–4} Subsequent work has shown that T[•], and its derivatives, are also powerful reagents for the selective oxidation of other functionalities such as carbohydrates^{5–9} and amines.^{10,11}

The catalytically active oxoammonium species (T⁺, Figure 1b) is simply generated by the one-electron oxidation of the inactive T[•] and reacts with alcohols resulting in an overall 2-proton/2-electron oxidation (dehydrogenation) process, as shown in Scheme 1.

Activation, and recycling, of this catalyst can be achieved by oxidation at electrodes^{1–4} or chemically either directly or

SCHEME 1: T[•]/T⁺ Oxidation of Alcohols



indirectly, with the deployment of secondary oxidation mediators (e.g., 2Br[•]/Br₂) that act along with primary molecular oxidants such as O₂ or H₂O₂.^{12–14} Obviously, since T[•]-mediated oxidations do not involve the usual metal-based reagents (e.g., the permanganates or chromates), it is considered to be a “green” approach to performing oxidations reactions;⁵ in particular, where the activation process is electrochemical, since it avoids the use of any ancillary redox reagents.

Unfortunately, irrespective of whichever activation procedure used, conversion of alcohols into carbonyl products via T[•]/T⁺ catalysis is usually deployed in molecular organic solvents such as acetonitrile;^{3,15–17} however, we,¹⁸ and others,¹⁹ have recently demonstrated the successful application of this catalytic system for the mediated electrochemical oxidation of alcohols in ionic liquid (IL) media. This is particularly advantageous since it represents the coupling of a “green”, recyclable, oxidizing reagent with “green” reaction media.^{20–22}

Although T[•]-mediated oxidations has been known for more than a quarter of a century, few mechanistic studies^{16,17,23–25} have appeared, and the exact mechanism has not yet been elucidated. However, it is known^{26–28} that there are at least two steps involved in the oxidation of alcohols by T⁺. First, it is assumed that T⁺ forms an intermediate adduct with the alcohol substrate; second, it is believed that the T⁺-alcohol adduct reacts, leading to the carbonyl compound and to one of the two reduced forms of T[•], i.e., either the hydroxylamine species (TH, Figure 1c) or its protonated form (TH₂⁺, Figure 1d).

* To whom correspondence should be addressed. E-mail: a.p.doherty@qub.ac.uk. Phone: +44 (0) 2890 974481. Fax: +44 (0) 28 9097 6524.

[†] Institut de Chimie et des Matériaux Paris Est.

[‡] Queen's University of Belfast.

Notwithstanding the lack of basic understanding of the reaction mechanism, it has been clearly established that the reaction is pH sensitive⁸ such that the reaction is very slow in the absence of base despite some studies reporting that the nature and concentration of the base has little influence on the reaction.²⁵ The catalytic effect of alkaline conditions is reasonable since the reaction involves the liberation of protons, and the availability of an ancillary proton “sink” (e.g., 2,6-lutidine (Lu) or HCO_3^-) is thermodynamically positive. Also, the liberation of protons, in the absence of an ancillary base, may lead to the thermodynamically favorable electron disproportionation reactions involving T^{\bullet} ^{29,30} as follows



These reactions are known to be complete and fast under acidic conditions and will lead to the inactivation of the $\text{T}^{\bullet}/\text{T}^+$ catalyst^{29,30} since TH and TH_2^+ are electrochemically inactive under acidic conditions. As such, the presence of base is necessary for the efficient deployment of T^{\bullet} as an alcohol oxidizing agent.

Although the base plays a key role as proton “sink” for the successful deployment of T^{\bullet} catalyst, its exact mechanistic role has yet to be elucidated. Obviously, in order to further develop and exploit this chemistry fully, a more detailed understanding of the role of the base in the reaction mechanism is desirable. This is of particular importance because T^{\bullet} , and other *N*-oxyl radicals, are attracting increasing attention due to their “green” credentials.⁵

The work described in this manuscript explores, in detail, the role of the base in T^{\bullet} -mediated oxidation of alcohols in *N*-butyl-*N*-methyl pyrrolidinium bistriflimide ([Bmpy][NTf₂]) IL. It will be shown here that the first step in the alcohol oxidation reaction involves a Brønsted equilibrium between the alcohol and the base, giving rise to the alcoholate ion, which is the reactive species oxidized by T^+ . It will also be shown that the same process occurs in molecular solvent environments.

Experimental Section

The IL used, [Bmpy][NTf₂], was prepared via ion metathesis in deionized water according to a literature procedure.³¹ ¹H and ¹³C NMR (Bruker Advance 300 MHz) spectra of the IL agreed with literature.

Electrochemical measurements were performed using a ParStat 2253 (Princeton Applied Research) potentiostat in the 3-electrode configuration. The working electrode was Au (area = 3.6×10^{-3} cm²), while Pt gauze acted as the counter electrode, and a Pt wire acted as a quasi-reference electrode. All potentials are quoted relative to the ferrocene/ferricinium (Fc/Fc⁺) redox couple recorded within the IL medium. The working electrode was polished with Emery 3/0 prior its use, and all measurements were performed at room temperature under an argon atmosphere.

Stock solutions of T^+ were prepared by bulk electrolyses of T^{\bullet} , which was performed in a divided cell fitted with a Nafion membrane¹⁸ in order to avoid parasitic reduction of T^+ . Typically, the anolyte volumes were 15 cm³ of the IL, which contained $2\text{--}4 \times 10^{-2}$ mol dm⁻³ of T^{\bullet} and the base. Catholyte volumes were typically 10 cm³ of IL + 5 cm³ of acetonitrile + 1 cm³ of water; the latter participated in the counter electrode reaction generating H₂. In this procedure, both the anode and cathode were platinum grids, while a Pt wire acted as a quasi-reference electrode. Electrolyses were performed at constant potential (0.45–0.55 V vs Fc/Fc⁺, i.e., 0.2–0.3 V vs E⁰_{T/T⁺})

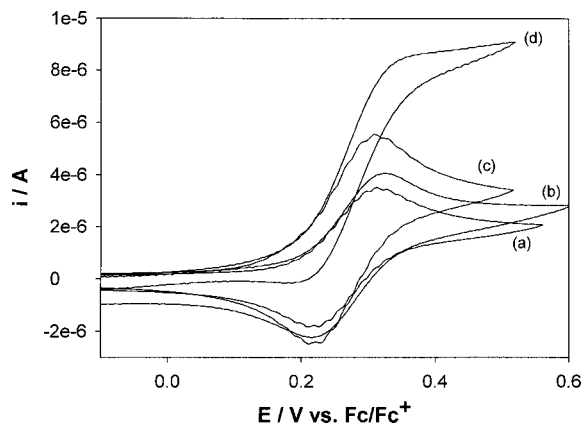


Figure 2. Cyclic voltammograms of (a) 0.042 mol dm⁻³ T^{\bullet} in [Bmpy][NTf₂] recorded at 0.1 V s⁻¹ along with (b) 0.56 mol dm⁻³ 3-phenylpropanol or (c) 1.27 mol dm⁻³ 2,6-lutidine. Curve d corresponds to a solution comprising of 0.042 mol dm⁻³ T^{\bullet} , 0.56 mol dm⁻³ 3-phenylpropanol, and 1.27 mol dm⁻³ 2,6-lutidine.

until either 1 F/mol (relative to [T^{\bullet}]) was passed or until the current decayed to near zero (i.e., <5% of the initial value).

Kinetic experiments were performed in a small electrochemical cell in the three electrodes configuration. Typically, a volume of 2 cm³ of the electrochemically prepared stock solution of $\text{T}^+ + \text{base}$ was used. A rotating platinum electrode (RDE) was used to record i_{Lim} vs time curves (chronoamperometry) where i_{Lim} is the diffusion-controlled limiting current due to the reduction of T^+ to T^{\bullet} at the RDE. To ensure this, the potential at the RDE was -0.1 V vs Fc/Fc⁺ (i.e., at > -300 mV reductive overpotential (vs E⁰_{T/T⁺}) thus ensuring fast heterogeneous electron transfer according to Butler–Volmer kinetics) whereupon addition of the alcohol (at time = t_0) initiated the T^+ reaction with alcohol, and hence, the recorded current decay transient is a direct measurement of T^+ consumption in the chemical reaction.

Results and Discussion

Cyclic Voltammetry (CV) of $\text{T}^{\bullet}/\text{T}^+$ -Mediated Oxidation of Alcohols. A cyclic voltammogram of T^{\bullet} in [Bmpy][NTf₂], recorded at a gold microelectrode, is shown in Figure 2a where the $\text{T}^{\bullet}/\text{T}^+$ redox couple exhibits a reversible one-electron redox process^{23,24,32–34} characterized by anodic and cathodic peak currents (i_{pa} and i_{pc} , respectively). Although it is well-known^{23,24,32–34} that $\text{T}^{\bullet}/\text{T}^+$ heterogeneous electron transfer is fast and reversible ($k^0 > 0.1$ cm s⁻¹), even in IL media,³² a recent publication³⁵ has shown that this is not the case in [Bmim][PF₆] (Bmim = 1-butyl-3-methylimidazolium) as IL. That the electrochemistry of $\text{T}^{\bullet}/\text{T}^+$ is reversible, and that the currents are diffusion controlled, in [Bmpy][NTf₂] was established with iR -compensated cyclic voltammetry measurements. These experiments showed that (1) the anodic–cathodic peak potential separation (ΔE_p) was independent of sweep rates (ν) up to 1 V s⁻¹ and (2) plots of anodic and cathodic peak currents vs $\nu^{1/2}$ were strictly linear up to 1 V s⁻¹. Collectively, these data clearly demonstrate that $\text{T}^{\bullet}/\text{T}^+$ redox is fast and diffusion controlled in [Bmpy][NTf₂] medium.

It can also be observed in Figure 2 that addition of either alcohol (3-phenylpropanol, Figure 2b) or base (Lu, Figure 2c) to the T^{\bullet} solution does not alter the voltammetry beyond the expected increase in peak currents due to the consequential decrease of the viscosity of the IL medium. In contrast, when 3-phenylpropanol and Lu are present together in the T^{\bullet} solution (Figure 2d), the reversibility of the $\text{T}^{\bullet}/\text{T}^+$ couple is lost, while

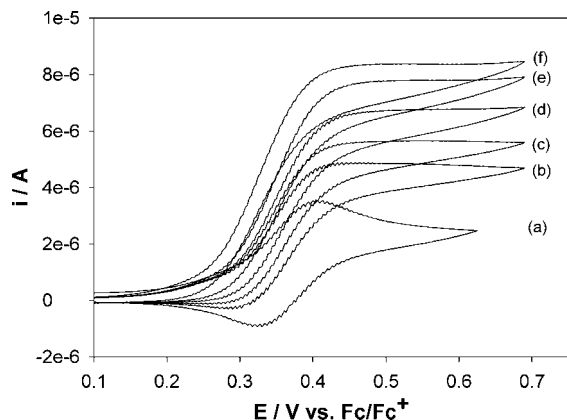


Figure 3. CV (30 mV s^{-1}) of (a) $4.10 \cdot 10^{-2} \text{ mol dm}^{-3} \text{ T}^*$ in [Bmpy][NTf₂] with $1.27 \text{ mol dm}^{-3} \text{ Lu}$ and with increasing 3-phenylpropanol concentrations of (b) 0.09, (c) 0.12, (d) 0.18, (e) 0.41, and (f) 0.78 mol dm^{-3} .

the anodic voltammetry exhibits a steady-state catalytic current (i_{cat}), which is independent of sweep-rate up to ca. 0.2 V s^{-1} . These observations are characteristic of T^*/T^+ redox catalysis where the electrochemical behavior of the T^*/T^+ system in [Bmpy][NTf₂] is similar to that observed in molecular organic solvents.^{8,18,30} Collectively, these data clearly demonstrate that in the absence of base the oxidation reaction is sufficiently slow as to be unobservable with CV at these time scales, whereas the presence of base catalyzes the mediated $2\text{e}^-/2\text{H}^+$ alcohol oxidation reaction.

For simple mediated electrochemical reactions, the rate of the mediator–substrate reaction, and hence the overall catalytic current, is known to follow second-order kinetics, i.e., first-order in terms of both substrate and mediator concentration. Indeed, the kinetic models proposed by Saveant³⁶ and by Nicholson and Shain³⁷ correspond to second-order and pseudo-first-order, conditions, respectively. However, it will be shown below that the mediated oxidation of alcohols by T^+ is not a simple second-order process but involves complex proton transfer step(s) such that catalytic currents are strongly dependent the nature of ancillary base, its concentration, and the concentration of its conjugate acid. As such, application of the conventional kinetic models^{36,37} is inappropriate for this reaction. The dependencies on alcohol concentration, base concentration, and type are examined qualitatively for the T^*/T^+ mediated oxidation of alcohol in ILs, as described below.

Parts a–f of Figure 3 show the evolution of the voltammetry with the progressive increase in alcohol concentration (3-phenylpropanol, from 0.09 to 0.78 mol dm^{-3}), at fixed T^* ($4.10 \cdot 10^{-2} \text{ mol dm}^{-3}$) and Lu (1.27 mol dm^{-3}) concentrations. It is clearly evident that increasing the alcohol concentration leads to an increase in the catalytic current and the loss of reversibility, as expected.

This alcohol concentration dependence is further demonstrated in Figure 4a where the ratios of $i_{\text{cat}}/i_{\text{pa}}$ (i_{pa} is the T^* oxidation peak current recorded in the absence of alcohol) are plotted as a function of 3-phenylpropanol concentration ([substrate]), at a constant T^* concentration ($4.1 \cdot 10^{-2} \text{ mol dm}^{-3}$) with a constant Lu concentration (0.28 mol dm^{-3}). It is, again, clearly evident that increasing the alcohol concentration increases the catalytic turnover but not in a first-order fashion. As noted above, there are no models available to quantitatively describe this effect.

The effect of increasing the Lu concentration ([substrate]) while maintaining a constant alcohol concentration (1.27 mol

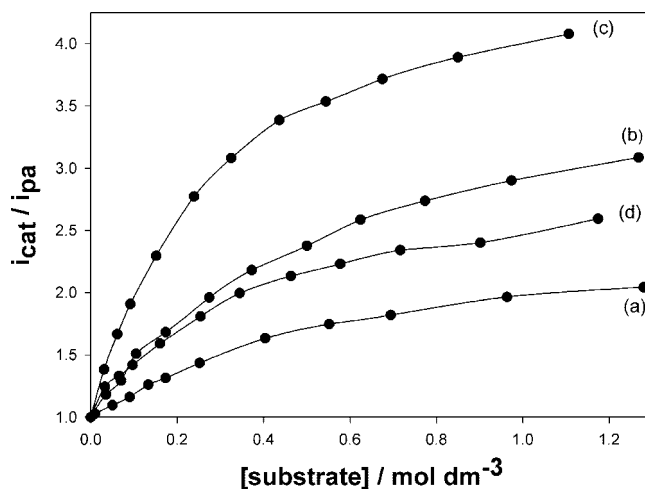


Figure 4. Solution of $4.10 \cdot 10^{-2} \text{ mol dm}^{-3} \text{ T}^*$ in [Bmpy][NTf₂]. Influence of (a) concentration of 3-phenylpropanol ([Lu] = 0.28 mol dm^{-3}) and concentration and nature of base ((b) Lu, (c) collidine, [alcohol] = 0.28 mol dm^{-3}) on the catalytic efficiency. Plot d corresponds to Lu addition accompanied by 10 mol % LuH^+ upon each addition.

dm^{-3}) is evident in Figure 4b, where it can be seen that increasing [Lu] to 1.27 mol dm^{-3} increases i_{cat} , as previously observed.⁸

Also, the effect of the $\text{p}K_{\text{a}}$ of the base can be seen by comparing Figure 4b with Figure 4c, which correspond to equivalent concentrations of Lu ($\text{p}K_{\text{a}} = 6.8$ in water) and collidine ($\text{p}K_{\text{a}} = 7.4$ in water), respectively, at a fixed alcohol concentration of 1.27 mol dm^{-3} . Obviously, the higher the $\text{p}K_{\text{a}}$ of the base the greater the catalytic efficiency observed. As far as we are aware, there are no other studies reporting the effect of the $\text{p}K_{\text{a}}$ of the ancillary base for this reaction.

Another approach to investigate the pH dependence of the reaction is to add the conjugate acid of the base (i.e., LuH^+ , as the CF_3SO_3^- salt) to the reaction medium. This is shown in Figure 4d where i_{cat} is plotted as a function of free [Lu] (exactly as in Figure 4b) but which is accompanied with 10 mol % of LuH^+ at each addition. It is immediately obvious that the conjugate acid acts as an inhibitor for the reaction.

To explore the influence of the conjugate acid further, the effect of the $[\text{LuH}^+]/[\text{Lu}]$ ratio on the cyclic voltammetry of T^*/T^+ was examined (with constant T^* and alcohol concentrations of $5 \cdot 10^{-2}$ and 0.28 mol dm^{-3} , respectively.) In these experiments, the initial concentration of Lu was 1.12 mol dm^{-3} whereupon $\text{CF}_3\text{SO}_3\text{H}$ was added to form LuH^+ (obviously, the mass-balance is $[\text{Lu}] + [\text{LuH}^+] = 1.12 \text{ mol dm}^{-3}$).

Part 1a of Figure 5 shows the cyclic voltammetry recorded in the absence of LuH^+ (where [Lu] was 1.12 mol dm^{-3}) and is simply the expected redox catalytic behavior as outlined above.

Part 1b of Figure 5 corresponds to the voltammetry recorded in the presence of $0.84 \text{ mol dm}^{-3} \text{ Lu}$ and $0.28 \text{ mol dm}^{-3} \text{ LuH}^+$ (i.e., $[\text{LuH}^+]/[\text{Lu}] = 0.33$), where it is evident that i_{cat} is significantly suppressed and that the T^*/T^+ couple begins to become reversible. It is also worth noting that this effect is the same, at constant $[\text{LuH}^+]/[\text{Lu}]$ ratio, irrespective of the overall base/conjugate acid concentrations. Part 1c of Figure 5 shows that increasing $[\text{LuH}^+]/[\text{Lu}]$ to 1 causes a further diminution of i_{cat} and enhancement of reversibility. Further augmentation of $[\text{LuH}^+]/[\text{Lu}]$ to 4.33 (part 1d of Figure 5) leads to completely reversible electrochemistry of the T^*/T^+ couple, i.e., redox catalysis no longer occurs at high $[\text{LuH}^+]/[\text{Lu}]$ ratios.

The effect of $[\text{LuH}^+]/[\text{Lu}]$ can be more clearly observed in part 2 of Figure 5 where i_{cat} is plotted as a function of $[\text{LuH}^+]/$

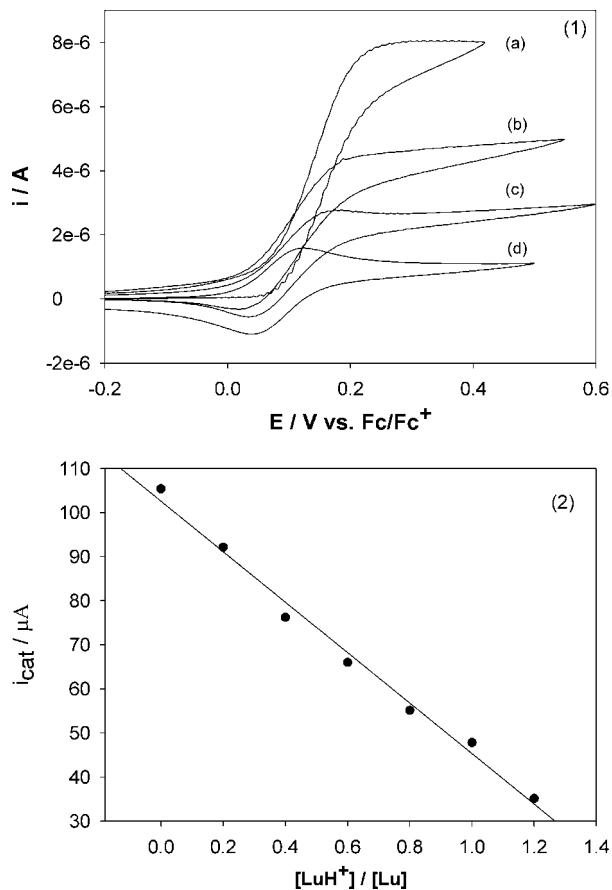


Figure 5. (1) CV (30 mV s^{-1}) of T^\bullet ($5 \times 10^{-2} \text{ mol dm}^{-3}$) in [Bmpy][NTf₂] with 3-phenylpropanol (0.28 mol dm^{-3}) and in the presence of Lu (mol dm^{-3})/LuH⁺ (mol dm^{-3}): (a) 1.12/0, (b) 0.84/0.28, (c) 0.56/0.56, and (d) 0.21/0.91. (2) Plot of i_{cat} vs addition $[LuH^+]/[Lu]$ where $([LuH^+] + [Lu]) = 1.0 \text{ mol dm}^{-3}$ and $[T^\bullet] = 4 \times 10^{-2} \text{ mol dm}^{-3}$ and $[3\text{-phenylpropanol}] = 1.27 \text{ mol dm}^{-3}$.

[Lu], which shows that i_{cat} decreases approximate linearly as a function of $[LuH^+]/[Lu]$ until $i_{cat} = i_{pa}$ when $[LuH^+]/[Lu] = 4.3$. This, again, clearly demonstrated the inhibitory effect of the conjugate acid.

Overall, Figures 1–5 demonstrate that the regeneration of the catalyst depends on the alcohol concentration, base concentration, the pK_a of the base, and the presence of the conjugate acid. From these observations, and the fact that the redox catalysis is not efficient in the absence of base, we can assume that there is an initial chemical step involving the alcohol and base which precedes the reaction of alcohol with the electrochemically generated T^+ . The simplest hypothesis is the occurrence of an acid–base equilibrium process generating the alcoholate species as given in eq 2



RDE Kinetic Investigation of T^+ Oxidation of Alcohols.

Although CV is a powerful method for investigating chemical reactions following electron transfer, it is informative to directly monitor the consumption of T^+ during the alcohol oxidation reaction, as a function of time, in an approach akin to classical chemical kinetics. In the following experiments, T^+ was initially fully electrolyzed to T^\bullet within the electrochemical cell. Obviously, upon subsequent addition of the alcohol substrate, T^+ is consumed. The diminution of T^+ concentration can be monitored amperometrically at a RDE poised at $-0.1 \text{ V vs } Fc/Fc^+$ due to

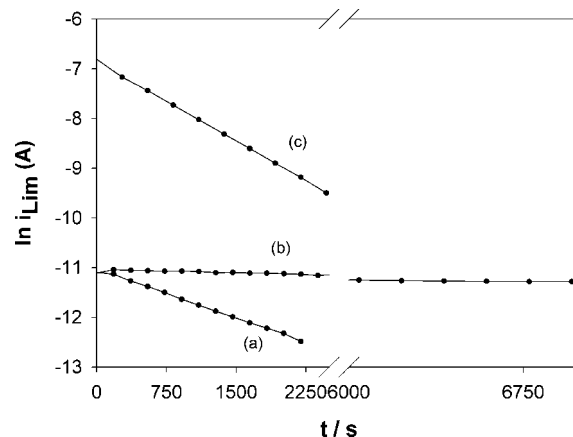


Figure 6. Plots of $\ln i_{Lim}$ vs time corresponding to the consumption of T^+ ($2.10^{-2} \text{ mol dm}^{-3}$) for the oxidation of (a) PhCH₂OH (0.4 mol dm^{-3}) and (b) Ph(CH₂)₃OH (0.4 mol dm^{-3}) in [Bmpy][NTf₂]. Curve c corresponds to PhCH₂OH (0.4 mol dm^{-3}) oxidation in acetonitrile under the same conditions.

the $T^+ + e^- \rightarrow T^\bullet$ reduction reaction. The resulting limiting current–time transients (i_{Lim}) can then be analyzed for chemical kinetic information in the usual manner. With this approach, it will be shown that alcohols do react with T^+ in the absence of base, albeit very slowly, which is unobservable with CV at the convenient sweep-rates described above.

Parts a and b of Figure 6 and show plots of $\ln i_{Lim}$ vs t (recorded at $-0.1 \text{ V vs } Fc/Fc^+$) following the addition of benzylic alcohol (a) and 3-phenylpropanol (b) (0.4 mol dm^{-3} in both cases) to T^+ solutions (initial concentration of T^+ was $2.10 \times 10^{-2} \text{ mol dm}^{-3}$) in [Bmpy][NTf₂] in the absence of base.

It is clearly evident that the alcohol oxidation reaction occurs in the absence of base and appears to be first order with respect to T^+ . For comparison, using the same conditions, Figure 6c shows $\ln i_{Lim}$ vs t following the addition of benzylic alcohol to T^+ in acetonitrile in the absence of base where first-order behavior is also observed. The half-lives under these three conditions (parts a–c of Figure 6) are estimated to be about 10^3 s , $2 \times 10^4 \text{ s}$, and $6 \times 10^2 \text{ s}$, respectively. Obviously, these reactions are sufficiently slow as to be unobservable in CV at convenient time scales, as noted above.

Obviously, the data presented above suggests that inclusion of base in the reaction medium accelerates alcohol oxidation reactions and allows the reactions to go to completion. These effect can be clearly seen in parts a and b of Figure 7, where 3-phenylpropan-1-ol and benzylic alcohol are observed to consume T^+ at approximately equivalent rates in the presence of Lu (in excess) in [Bmpy][NTf₂] medium. Figure 7c shows the consumption of T^+ upon addition of 3-phenylpropan-1-ol where Lu has been replaced with picoline. It is clear that the reaction rate is faster for Lu than for picoline, which is a reflection of their relative pK_a s, i.e., (Lu $pK_a = 6.8$, picoline $pK_a = 5.7$ in water).

These results are in complete agreement with those obtained by CV, which, collectively, suggest that the rate of reaction between T^+ and alcohol depends on an acid–base equilibrium process (eq 2) generating the active alcoholate species.

To establish if alcoholate is readily oxidizable by T^+ , an experiment was conducted where the alcoholate, PhCH₂O⁻ (prepared in THF from PhCH₂OH and sodium) was added to a T^+ solution. Under these conditions, the consumption of T^+ was instantaneous such that the chronoamperometric response was a step function rather than measurable kinetic-controlled

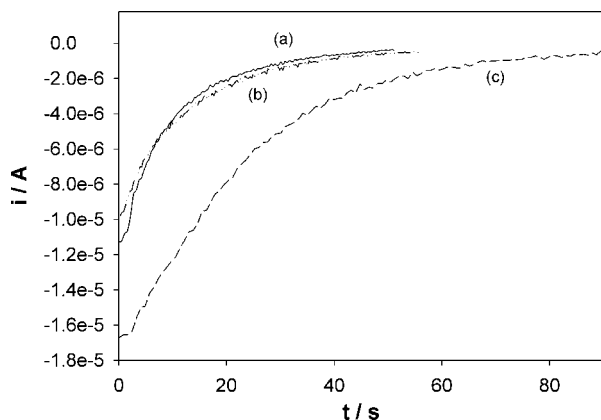


Figure 7. Chronoamperograms of T^+ consumption (initial T^+ $2 \times 10^{-2} \text{ mol dm}^{-3}$) in [Bmpy][NTf₂] under the following conditions: (a) 0.12 mol dm^{-3} 3-phenylpropanol + 0.14 mol dm^{-3} Lu, (b) 0.12 mol dm^{-3} benzyl alcohol + 0.14 mol dm^{-3} Lu, and (c) 0.12 mol dm^{-3} 3-phenylpropanol + 0.14 mol dm^{-3} picoline.

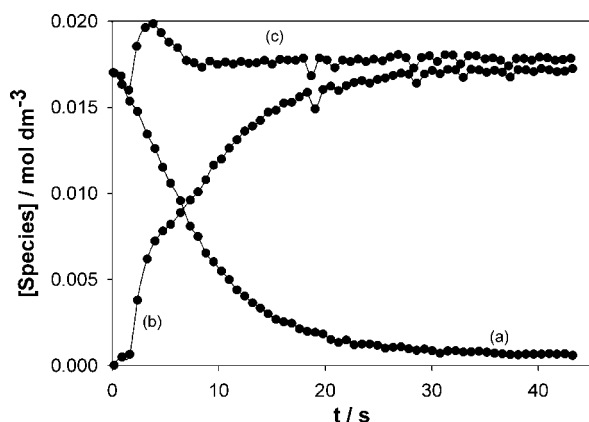
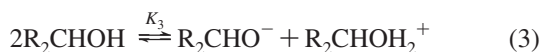


Figure 8. Plots of (a) T^+ consumption, (b) T^* regeneration, and (c) $T^+ + T^*$ mass balance. Initial conditions were 0.12 mol dm^{-3} Ph(CH₂)₃OH, 0.38 mol dm^{-3} [Lu], and $1.7 \times 10^{-2} \text{ mol dm}^{-3}$ T^+ in [Bmpy][NTf₂].

decay transience. This strongly indicates that the overall oxidation reaction is controlled by the equilibrium in eq 2.

Conversely, in absence of base, the pre-equilibrium generating the alcoholate could be the autoprotolysis of the alcohol according to eq 3



Compared to lutidine or picoline, the weak basicity of the alcohol leads only to an extremely low equilibrium concentration of alcoholate ($K_3 \ll K_2$), and consequently, the very slow reaction rate observed.

It is also vital to know the fate of T^+ as it reacts with the alcohol since this knowledge will be used later in the development of a kinetic model for the reaction. The expected disappearance of T^+ , as a function of time, is shown in Figure 8a, while Figure 8b charts the concomitant reappearance of T^* (recorded by chronoamperometry at a RDE electrode at 0.45 to 0.55 V vs Fc/Fc⁺). Figure 8c shows the corresponding mass balance for T^+ consumption and T^* reformation. Obviously, T^+ fully returns to T^* during the reaction. It is also important to note that T^* regeneration occurs at the same rate as T^+ disappearance.

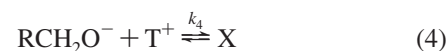
Reaction Mechanism and Kinetic Model. The observations made above lead to the following proposed mechanism and

TABLE 1: Mass Balance for Various Species Involved in the Overall Oxidation Reaction along with Their Abbreviations at the Beginning of the Experiment ($t = 0$) and during the Experiment ($t = t_x$)

$RCH_2OH +$	$2T^+ +$	$2B \rightarrow$	$RCHO +$	$2BH^+ +$	$2T^*$
$[Alc]_0$	$[T^+]_0$	$[B]_0$	0	a^a	0
$[Alc]_0 - x/2$	$[T^+]_0 - x$	$[B]_0 - x$	$x/2$	$a + x$	x

^a The initial amount of BH^+ (a) was measured by acid base titration of a sample of the electrolytic solution after electrogeneration of T^+ or was chosen at will by partial neutralization of B with a strong acid (e.g., CF₃SO₃H).

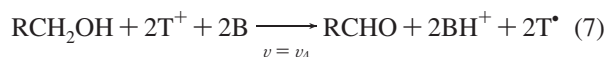
kinetic model. Here, the initial pre-equilibrium between the alcohol and base (eq 2) allows generation of the active alcoholate species and the conjugate acid (BH^+). The alcoholate reacts with T^+ to form an adduct X (eq 4), which then reacts with another B and another T^+ , giving the carbonyl product, conjugated acid, and $2 T^*$ (eq 5)



The observation that the rate of T^* regeneration is equivalent to T^+ consumption (parts a–c of Figure 8) demonstrates that the steps involved in eq 5 are faster than the steps involved in eq 4. Consequently, the experimentally observed consumption of T^+ corresponds to the superposition of eqs 4 and 5



The global balance of the reaction can therefore be written as eq 7, with a global rate (ν) equal to the rate of eq 4, ν_4 , i.e., $\nu = \nu_4$



Consequently, we can write

$$\nu_4 = k_4[T^+][RCH_2O^-] \text{ with } [RCH_2O^-] = \frac{K_2[RCH_2OH][B]}{[BH^+]} \quad (8)$$

According to the stoichiometry of eq 6, the rate of disappearance of T^+ ($d[T^+]/dt$), as measured at the RDE, is therefore equal to $2\nu_4$.

The mass balance for the various species involved in the overall oxidation reaction (eq 6), along with their abbreviations at the beginning of the experiment ($t = 0$) and during the experiment ($t = t_x$), are given in Table 1.

Also, the equilibrium in eq 2 implies that the steady-state concentration of RCH_2O^- is

$$[RCH_2O^-] = \frac{K_2([Alc]_0 - x/2)([B]_0 - x)}{a + x} \quad (9)$$

The global rate of eqs 6 (and/or eq 7) can be expressed as

$$\nu_4 = k_4[RCH_2O^-][T^+] = -\frac{1}{2} \frac{d[T^+]}{dt} \quad (10)$$

or by

$$v_4 = -\frac{1}{2} \frac{d([T^+]_0 - x)}{dt} = \frac{1}{2} \frac{dx}{dt} \quad (11)$$

where dx/dt is

$$\frac{dx}{dt} = 2k_4K_2 \left([Alc]_0 - \frac{x}{2} \right) ([B]_0 - x) \frac{1}{a+x} ([T^+]_0 - x) \quad (12)$$

Defining $k' = 2k_4K_2([Alc]_0 - x/2)([B]_0 - x)$ leads to

$$k' dt = \frac{a+x}{([T^+]_0 - x)} dx \quad (13)$$

Keeping $[T^+]$ low relative to $[Alc]$ and $[B]$ (e.g., under catalytic conditions) ensures that $[Alc]_0 - x/2 \approx [Alc]_0$ and $[B]_0 - x \approx [B]_0$, it then follows that k' is almost constant, and is given by

$$k' \approx 2k_4K_2[Alc]_0[B]_0 \quad (14)$$

Finally, integration of eq 12 above leads to

$$(a + [T^+]_0) \ln([T^+]_0 - x) + x = -k't + (a + [T^+]_0) \ln([T^+]_0) \quad (15)$$

Equation 15 accounts for all the qualitative observations made with CV and RDE outlined above, and as will be shown below, also accounts quantitatively for the kinetic behavior observed experimentally and therefore yields values for the kinetic (k_4) and equilibrium (K_2) parameters, since all the other terms in the equation are known.

Model Testing. Now, experimental i_{Lim} vs t data, recorded during the course of the reaction, can be converted into plots of $(a + [T^+]_0) \ln([T^+]_0 - x) + x$ vs time (t , eq 15), since i_{Lim} , at the beginning of the experiment, yields $[T^+]_0$ and, due to mass balance (cf. parts a–c of Figure 8), the change in I_{Lim} during the course of the experiment gives x over time, and a is known at the outset.

Parts a–c of Figure 9 show three examples of such plots obtained either with aliphatic (3-phenyl propan-1-ol, parts a and c of Figure 9) or benzylic (Figure 9b) alcohols in the presence of either Lu (Figure 9a and 9b) or pyridine (Figure 9c). (Note that in these experiments $[T^+] \ll [Alc]_0$ and $[B]_0$ to ensure eq 14 is valid). The slight nonlinearity at the beginning and the end of the experiment is due to initial mixing and low signal/noise ratio at the end of the reaction (as $i_{Lim} \rightarrow 0$), respectively. Otherwise, the plots are linear ($r^2 > 0.99$) and agree well with

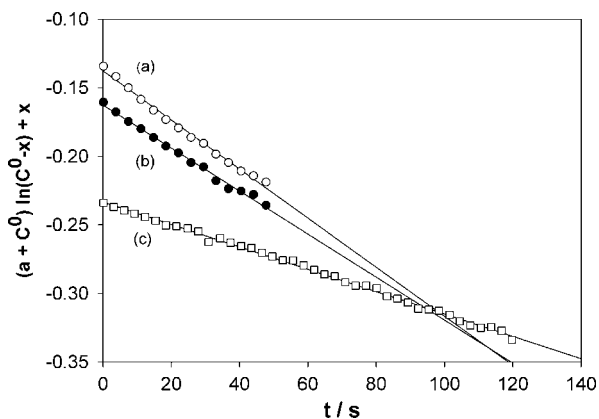
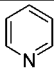
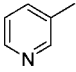
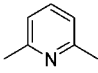
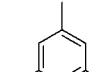


Figure 9. Kinetic plots obtained in [Bmpy][NTf₂] for (a) 0.12 mol dm⁻³ Ph(CH₂)₃OH/0.14 mol dm⁻³ Lu/1.8 × 10⁻² mol dm⁻³ T⁺/1.8 × 10⁻² mol dm⁻³ LuH⁺, (b) 0.12 mol dm⁻³ PhCH₂OH/0.14 mol dm⁻³ Lu/9 × 10⁻³ mol dm⁻³ T⁺/2.5 × 10⁻² mol dm⁻³ [LuH⁺], and (c) 0.12 mol dm⁻³ Ph(CH₂)₃OH, 0.42 mol dm⁻³ pyridine/4.1 × 10⁻² mol dm⁻³ PyH⁺.

TABLE 2: Kinetic Data Obtained in [Bmpy][NTf₂] at Various 3-Phenylpropan-1-ol, Lutidine, and Conjugate Acid Concentrations with 2.0 × 10⁻² mol dm⁻³ T⁺

entry	[Alc] ₀ (mol dm ⁻³)	[Lu] ₀ (mol dm ⁻³)	[LuH ⁺] ₀ (mol dm ⁻³)	k ₄ K ₂ (dm ³ mol ⁻¹ s ⁻¹)
1	0.12	0.14	1.8 × 10 ⁻²	7 × 10 ⁻²
2	0.12	0.43	4.3 × 10 ⁻²	1 × 10 ⁻¹
3	0.12	0.43	0.13	1.2 × 10 ⁻¹
4	0.12	0.43	0.43	1.4 × 10 ⁻¹
5	0.24	0.14	3.1 × 10 ⁻²	9 × 10 ⁻²

TABLE 3: Kinetic Data in [Bmpy][NTf₂] for 3-Phenylpropan-1-ol (0.12 mol dm⁻³) Oxidation in the Presence of Various Bases^a

entry	base	pK _a in H ₂ O	k ₄ K ₂ dm ³ mol ⁻¹ s ⁻¹
1	 pyridine	5.25	9.5 × 10 ⁻³
2	 3-picoline	5.7	1.4 × 10 ⁻²
3	 2,6-lutidine	6.75	1.0 × 10 ⁻¹
4	 2,4,6-collidine	7.43	≈ 1 (estimation)

^a The concentration T⁺ was 2.0 × 10⁻² mol dm⁻³, and all base concentrations were 0.41 mol dm⁻³, while the conjugate acid concentrations were 5.0 × 10⁻² mol dm⁻³.

the kinetic model outlined above. Obviously, the kinetic term $k' (2k_4K_2[Alc]_0[B]_0)$ can be obtained from the slopes of the regression lines (solid lines) in parts a–c of Figure 9.

Further confirmation of the correctness of the model can be obtained from the data in Tables 2 and 3. The data in Table 2 corresponds to the oxidation of 3-phenylpropan-1-ol in the presence of Lu and LuH⁺ at various mole ratios. Now, although the rate of the reaction depends on the concentration of each of the three compounds, it can be seen that the value of the product k_4K_2 , which depends only on the nature of the base and the alcohol, is almost constant (mean value ≈ 10⁻¹ dm³ mol⁻¹ s⁻¹), which agrees with the proposed mechanism.

The data in Table 3 concerns 3-phenylpropan-1-ol oxidation in the presence of various bases along with their respective conjugated acids. It is evident that the value of the kinetic term (k_4K_2) increases with the strength of the base. In particular, comparison of k_4K_2 values for entries 2 and 3 in Table 3 is informative since the ratio of the respective kinetic terms is ca. 10, what agrees fully with the unit difference between the respective pK_a values (in water) of the two bases.

By consideration of the observation evident in Figure 9 and the data in Tables 2 and 3, the proposed mechanism and kinetic model account well for the effect of initial concentrations of the alcohol and base, the pK_a of the bases and the presence of the conjugate acid.

Evaluation of k_4 . The rate parameter k_4K_2 describing the rate of the alcohol oxidation reaction is the product of the rate constant of eq 4 and the acid–base equilibrium constant of eq 2. Referring to pK_a values in water (16 for a primary alcohol

TABLE 4: Rate Constants for T⁺-Mediated Electro-Oxidations of Alcohols in [Bmpy][NTf₂]

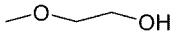
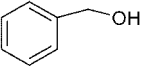
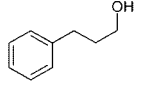
Alcohol	[T ⁺] (x 10 ⁻³ mol dm ⁻³)	[alcohol] (x 10 ⁻³ mol dm ⁻³)	[Lu] (x 10 ⁻³ mol dm ⁻³)	k ₄ K ₂ (dm ³ mol ⁻¹ s ⁻¹)	k ₄ dm ³ mol ⁻¹ s ⁻¹
	20	400	14	0.10	1.0 x 10 ⁸
	15	120	14	0.09	0.9 x 10 ⁸
	14	240	14	0.10	1.0 x 10 ⁸

TABLE 5: Kinetic Data for 3-Phenylpropan-1-ol Oxidation in Acetonitrile or [Bmpy][NTf₂] with 0.02 mol dm⁻³ T⁺ and Various Bases

entry	[alcohol] ₀ (mol dm ⁻³)	base and cion (mol dm ⁻³)	solvent	k ₄ K ₂ (dm ³ mol ⁻¹ s ⁻¹)
1	0.12	pyridine (0.42)	bmpyNTf ₂	9.5 × 10 ⁻³
2			MeCN	1.6 × 10 ⁻³
3	0.12	2,6-lutidine (0.39)	bmpyNTf ₂	9.0 × 10 ⁻²
4			MeCN	1.4 × 10 ⁻²
5	0.24	2,6-lutidine (0.14)	bmpyNTf ₂	9.0 × 10 ⁻²
6			MeCN	1.4 × 10 ⁻²

and 7 for lutidine), K_2 for Lu/alcohol equilibrium is 1×10^{-9} , and hence, k_4 for eq 4 can be approximated. These values are given in Table 4 for the three primary alcohols used and are found to be approximately $1 \times 10^8 \text{ dm}^3 \text{ mol}^{-1} \text{ s}^{-1}$. The remarkably high value for this term supports the observation made above that alcoholate reacts “instantaneously” with T⁺. It is also noteworthy that k_4 values are essentially independent of [T⁺], [alcohol], [Lu], and the nature of the alcohol. This observation indicates that the rate of T⁺ oxidation of alcohols is controlled entirely by the initial acid–base equilibrium described in eq 2. As such, the key to deploying T⁺ redox catalysts efficiently is the adoption of strong bases to favor the equilibrium in eq 2.

Comparison with Oxidation in Acetonitrile. Kinetic measurements and data analysis were performed in the same way as for that shown in parts a–c of Figure 9 where acetonitrile (containing 0.2 mol dm⁻³ LiNTf₂ as electrolyte) replaced the IL medium. Identical behavior was observed under these conditions, which suggests that the proposed mechanism and kinetic model are also valid in molecular solvent media. Also, as evident in Table 5, k_4K_2 were always larger (by a factor of 6) in IL than in MeCN, which clearly demonstrates that the reaction of T⁺ with alcohol (and concomitant regeneration of T⁺) is somewhat faster in IL. The origin of this difference is unclear; however, it seems to indicate that k_4 and/or K_2 is somewhat influenced by the nature of the reaction medium.

Conclusions

The mechanism of the redox catalytic oxidation of alcohols by T⁺ in an IL medium has been investigated using CV and RDE voltammetry. It has been shown that the rate of reaction and the contemporaneous rate of catalyst (T⁺) regeneration depend on the alcohol concentration, base concentration, the pK_as of the base and alcohol, and the presence of the conjugate acid. A kinetic model, founded on these observations, is proposed where the initial step in the reaction is a pre-equilibrium involving the formation of the alcoholate species through acid–base equilibrium with the base, the equilibrium constant (K) of which is shown to control the overall rate of the reaction. As such, development of rapid synthetic procedures using T⁺ requires the use of strong bases.

The proposed model also accounted for the reaction kinetics observed in polar solvent (acetonitrile), which indicates that the reactions proceed, mechanistically at least, equivalently in either environments. It was also observed that the product k_4K was a factor of ca. 6 larger in IL than in acetonitrile, which is probably a function of differing K in either environment.

Acknowledgment. The authors thank the COSTD29 Programme for funding. S.O. thanks Queen’s University for a Studentship.

References and Notes

- (1) Semmelhack, M. F.; Chou, C. S.; Cortés, D. A. *J. Am. Chem. Soc.* **1983**, *105*, 4492–4494.
- (2) Palmisano, G.; Ciriminna, R.; Pagliaro, M. *Adv. Synth. Catal.* **2006**, *348*, 2033–2037.
- (3) Deronzier, A.; Limosin, D.; Moutet, J. M. *Electrochim. Acta* **1987**, *32*, 1643–1647.
- (4) Liaigre, D.; Breton, T.; Belgsir, E. M. *Electrochem. Commun.* **2005**, *7*, 312–316.
- (5) Merbouh, N.; Bobbitt, J. M.; Brückner, C. *Organic Prep. Proc. Int.* **2004**, *36*, 1–31.
- (6) Breton, T.; Bashiardes, G.; Léger, J. M.; Kokoh, K. B. *Eur. J. Org. Chem.* **2007**, 1567–1570.
- (7) Barbier, M.; Breton, T.; Servat, K.; Grand, E.; Kokoh, B.; Kovensky, J. *J. Carbohydr. Chem.* **2006**, *25*, 253–266.
- (8) Schnatbaum, K.; Schäfer, H. J. *Synthesis* **1999**, *5*, 864–872.
- (9) Schämman, M.; Schäfer, H. J. *Eur. J. Org. Chem.* **2003**, 351–358.
- (10) Kashiwagi, Y.; Anzai, J. I. *Chem. Pharm. Bull.* **2001**, *49*, 324–326.
- (11) Fields, J. D.; Kropp, P. J. *J. Org. Chem.* **2000**, *65*, 5937–5941.
- (12) Jiang, N.; Ragauskas, A. *Tetrahedron Lett.* **2005**, *46*, 3323–3326.
- (13) Jiang, N.; Ragauskas, A. *Org. Lett.* **2005**, *7*, 3689–3692.
- (14) Ansari, I. A.; Gree, R. *Org. Lett.* **2002**, *4*, 1507–1509.
- (15) Zhao, M.; Li, J.; Mano, E.; Song, Z.; Tschäen, D. M.; Grabowski, E. J. J.; Reider, P. J. *J. Org. Chem.* **1999**, *64*, 2564–2566.
- (16) Kashiwagi, Y.; Uchiyama, K.; Kurashima, F.; Kikuchi, C.; Anzai, J. I. *Chem. Pharm. Bull.* **1999**, *47*, 1051–1052.
- (17) Kashiwagi, Y.; Uchiyama, K.; Kurashima, F.; Kikuchi, C.; Anzai, J. I. *Chem. Pharm. Bull.* **1999**, *47*, 1051–1052.
- (18) Barhdadi, R.; Commings, C.; Doherty, A. P.; Nédélec, J. Y.; O’Toole, S.; Troupel, M. *J. Appl. Electrochem.* **2007**, *37*, 723–728.
- (19) Kuroboshi, M.; Fujisawa, J.; Tanaka, H. *Electrochemistry* **2004**, *12*, 846–848.
- (20) Welton, T. *Chem. Rev.* **1999**, *99*, 2071–2083.
- (21) *Ionic Liquids in Synthesis*; Wasserscheid, P., Welton, T., Eds.; Wiley-VCH: Weinheim, Germany, 2003.
- (22) Earle, M. J.; Seddon, K. R. *Pure Appl. Chem.* **2000**, *72*, 1391–1398.

- (23) Kishioka, S. Y.; Yamada, A. *Electrochim. Acta* **2006**, *51*, 4582–4588.
- (24) Kishioka, S. Y.; Yamada, A. *J. Electroanal. Chem.* **2005**, *578*, 71–77.
- (25) Kishioka, S. Y.; Ohki, S.; Ohsaka, T.; Tokuda, K. *J. Electroanal. Chem.* **1998**, *452*, 179–186.
- (26) Ganem, B. *J. Org. Chem.* **1975**, *40*, 1998–2000.
- (27) Semmelhack, M. F.; Schmid, C. R.; Cortés, D. A. *Tetrahedron Lett.* **1986**, *27*, 1119–1122.
- (28) Yamaguchi, M.; Takata, T.; Endo, T. *J. Org. Chem.* **1990**, *55*, 1490–1492.
- (29) Golubev, V. A.; Sen, V. D.; Kulyk, I. V.; Aleksandrov, A. L. *Bull. Acad. Sci. USSR Chem. Ser.* **1975**, *24*, 2119–2126.
- (30) Kishioka, S. Y.; Ohsaka, T.; Tokuda, K. *Electrochim. Acta* **2003**, *48*, 1589–1594.
- (31) MacFarlane, D. R.; Meakin, P.; Sun, J.; Amini, N.; Forsyth, M. *J. Phys. Chem. B* **1999**, *103*, 4164–4170.
- (32) Evans, R. G.; Wain, A. J.; Hardacre, C.; Compton, R. G. *Chem. Phys. Chem.* **2005**, *6*, 1035–1039.
- (33) Summermann, W.; Deffner, U. *Tetrahedron* **1975**, *31*, 593–596.
- (34) Kishioka, S. Y.; Yamada, A. *Electrochim. Acta* **2005**, *51*, 462–466.
- (35) Herath, A. J.; Becker, J. Y. *Electrochim. Acta* **2008**, *53*, 4324–4330.
- (36) Saveant, J. M.; Vianello, E. *Advances in Polarography*; Longmuir, I. S., Ed.; Pergamon Press, New York, 1960; Vol. I, p 367
- (37) Nicholson, R. S.; Shain, I. *Anal. Chem.* **1964**, *35*, 706–723.

JP801253N